


ORIGINAL ARTICLE

Dhx15 regulates zebrafish definitive hematopoiesis through the unfolded protein response pathway

Yuanhua Cai¹ | Jing Wang¹ | Daqing Jin² | Qiao Liu¹ | Xianglei Chen¹ | Lili Pan^{1,3} | Yang Li^{1,3} | Xuechun Wang¹ | Feng Qian⁴ | Jiucun Wang⁴ | Tao Peter Zhong^{2,5} | Shaoyuan Wang^{1,3} 

¹Union Clinical Medical Colleges, Fujian Medical University, Fuzhou, China

²Shanghai Key Laboratory of Regulatory Biology, Institute of Molecular Medicine, East China Normal University School of Life Sciences, Shanghai, China

³Department of Hematology, Fujian Institute of Hematology, Fujian Provincial Key Laboratory on Hematology, Fujian Medical University Union Hospital, Fuzhou, China

⁴School of Life Sciences and Institutes of Biomedical Sciences, Ministry of Education Key Laboratory of Contemporary Anthropology and State Key Laboratory of Genetic Engineering, Collaborative Innovation Center for Genetics and Development, Fudan University, Shanghai, China

⁵Department of Medicine, Vanderbilt University School of Medicine, Nashville, TN, USA

Correspondence

Shaoyuan Wang, Department of Hematology, Fujian Institute of Hematology, Fujian Provincial Key Laboratory on Hematology, Fujian Medical University Union Hospital, Fuzhou, China.
Email: shaoyuanwang@fjmu.edu.cn

Tao Peter Zhong, Shanghai Key Laboratory of Regulatory Biology, Institute of Molecular Medicine, East China Normal University School of Life Sciences, Shanghai, China.
Email: tzhong@bio.ecnu.edu.cn

Funding information

National Natural Science Foundation of China, Grant/Award Number: 81770163, 81270609, 81470008 and 81500139; Fujian Province Health Education Joint Research Project, Grant/Award Number: 2016-2-07; Fujian Provincial Department of Finance, Grant/Award Number: 2017-655; Construction Project of Fujian Medical Center of Hematology, Grant/Award Number: 201704; The National and Fujian Provincial Key Clinical Specialty Discipline Construction Program, Grant/Award Number: 2011-1006 and 2012-149

Abstract

Gene alterations are recognized as important events in acute myeloid leukemia (AML) progression. Studies on hematopoiesis of altered genes contribute to a better understanding on their roles in AML progression. Our previous work reported a DEAH box helicase 15 (DHX15) R222G mutation in AML patients, and we showed DHX15 overexpression is associated with poor prognosis in AML patients. In this work, we further study the role of *dhx15* in zebrafish developmental hematopoiesis by generating *dhx15*^{-/-} zebrafish using transcription activator-like effector nuclease technology. Whole-mount in situ hybridization (WISH) analysis showed hematopoietic stem/progenitor cells were dramatically perturbed when *dhx15* was deleted. Immunofluorescence staining indicated inhibited hematopoietic stem/progenitor cell (HSPC) proliferation instead of accelerated apoptosis were detected in *dhx15*^{-/-} zebrafish. Furthermore, our data showed that HSPC defect is mediated through the unfolded protein response (UPR) pathway. DHX15 R222G mutation, a recurrent mutation identified in AML patients, displayed a compromised function in restoring HSPC failure in *dhx15*^{-/-}; Tg (*hsp: DHX15 R222G*) zebrafish. Collectively, this work revealed a vital role of *dhx15* in the maintenance of definitive hematopoiesis in zebrafish through the unfolded protein response pathway. The study of DHX15 and

Abbreviations: 4-PBA, 4-phenylbutyric acid; AML, acute myeloid leukemia; ATF, activating transcription factor; CHT, caudal hematopoietic tissue; DHX15, DEAH box helicase 15; dpf, days post fertilization; ER, endoplasmic reticulum; hpf, hours post fertilization; HS, heat-shocked at 38°C for 1 h and 45 min once a day after 25 hpf; HSC, hematopoietic stem cell; HSPC, hematopoietic stem/progenitor cell; IRE1, inositol-requiring protein-1; PBST, PBS with 0.3% Triton X-100; PERK, protein kinase RNA (PKR)-like ER kinase; pH3, phospho-histone H3; qRT-PCR, quantitative real-time PCR; TALEN, transcription activator-like effector nucleases; UPR, unfolded protein response; VDA, ventral wall of dorsal aorta; XBP1, X-box binding protein 1; WISH, whole-mount in situ hybridization.

Cai and Wang are contributed equally to this work.

This is an open access article under the terms of the Creative Commons Attribution-NonCommercial-NoDerivs License, which permits use and distribution in any medium, provided the original work is properly cited, the use is non-commercial and no modifications or adaptations are made.

© 2021 The Authors. *Cancer Science* published by John Wiley & Sons Australia, Ltd on behalf of Japanese Cancer Association.

DHX15 R222G mutation could hold clinical significance for evaluating prognosis of AML patients with aberrant DHX15 expression.

KEYWORDS

acute myeloid leukemia, DEAH box helicase 15, hematopoiesis, unfolded protein response, zebrafish

1 | INTRODUCTION

Acute leukemia is a dangerous blood disorder characterized by impaired differentiation and increased proliferation of immature blood cells. The occurrence and progression of acute leukemia are usually accompanied by somatic gene alterations. Accumulating gene alterations have been extensively studied in acute leukemia development. The roles of some altered genes (*IDH*, *FLT3*, and *NPM1*) are well established on developmental hematopoiesis,¹⁻³ which contribute to a profound understating of those genes during the occurrence and progression of AML. Our previous study reported DHX15 R222G mutation in a Chinese family with AML and some sporadic AML patients.⁴ The same mutation has been reported in AML patients by other groups.⁵⁻¹⁰ Our study found DHX15 is upregulated and associated with poor outcomes, which indicates the importance of DHX15 and DHX15 R222G in AML pathogenesis. But the role of DHX15 and its R222G mutation on developmental hematopoiesis remain exclusive.

DHX15 is a member of DExH/D RNA helicase, which is presented in different processes involving RNA metabolism. PRP43, a yeast homologous protein of DHX15, dismantles the intron-lariat spliceosome into the dissociative lariat during pre-mRNA splicing.¹¹ In ribosome biogenesis, PRP43 implicated in ribosomal RNA and snoRNA responses.^{12,13} Recent studies indicate DHX15 correlates with cancer development.¹⁴⁻¹⁶ Studies by Xu et al¹⁷ and Jing et al¹⁵ revealed the roles of DHX15 in prostate progression. DHX15 is upregulated in castration-resistant prostate cancer by interacting with the androgen receptor.^{15,17} DHX15 overexpression is also found in hepatocellular carcinoma and is associated with an aggressive phenotype of cancer.¹⁶ Lin et al¹⁴ revealed DHX15 induces a growth-promoting effect on mammalian cells by increasing ATPase activity through DHX15 and G-patch domain containing 2 interaction. These studies indicate that, in addition to the roles in RNA metabolism, DHX15 plays an important role in the pathogenesis of cancer.

In recent decades, zebrafish has emerged as a model organism for hematopoietic study. Zebrafish share highly conserved key genetic factors, cell types, and hematopoiesis development with humans. Zebrafish hematopoiesis undergoes two successive waves. Primitive hematopoiesis originates from anterior lateral plate mesoderm and intermediate cell mass, which mainly produce primary macrophages and erythrocytes, respectively.¹⁸ During definitive hematopoiesis, HSPCs emerged from the VDA (aorta-gonad-mesoderm in mammals)¹⁹ at approximately 24 hpf.²⁰ Hematopoietic stem/progenitor

cells migrate to CHT (fetal liver in mammals) at 48 hpf.²¹ Colonization of HSPCs at CHT ensure expansion and differentiation of HSPCs.²² By 3 dpf, lymphopoiesis initiates in the thymus.¹⁹ Finally, HSPCs gradually colonize the kidney (bone marrow in mammals), a long-term hematopoietic site in adult zebrafish after 5 dpf.¹⁹

Here, we built upon our previous study and further explore the role of DHX15 in developmental hematopoiesis. We generated *dhx15*^{-/-} zebrafish and conditionally overexpressed DHX15/DHX15 R222G transgenic zebrafish. Our study found *dhx15* plays a prominent role in zebrafish definitive hematopoiesis through the UPR pathway. Failure of HSPCs is caused by inhibited proliferation of HSPCs in CHT. DHX15 R222G, the mutation identified in AML patients, is limited in restoring HSPC failure in *dhx15*^{-/-} zebrafish compared with DHX15. Thus, our study revealed a novel and vital role of *dhx15* in definitive hematopoiesis in zebrafish. DHX15 R222G mutation could play an important role in the pathogenesis of leukemia.

2 | MATERIALS AND METHODS

2.1 | Zebrafish strains and husbandry

Zebrafish stock were raised and kept under standard laboratory conditions at 28.5°C. AB wild-type, *Tg(cmyb:gfp)* zebrafish,²³ and *Tg(flk:egfp)* zebrafish²⁴ were used in this study. *Dhx15*^{+/-}; *Tg(flk:egfp)* zebrafish were generated by crossing *dhx15*^{+/-} with *Tg(flk:egfp)* zebrafish. This study was carried out according to the Guide for the Care and Use of Laboratory Animals from the NIH. Experiments involving zebrafish were approved by the Institutional Animal Care and Use Committee, Fudan University.

2.2 | Generation of *dhx15*^{-/-} zebrafish

Genome information for zebrafish *dhx15* (NC_007118.7) was obtained from the NCBI. The left arm (ATAAAGAGCGCTTTAAT) and right arm (CAGAGCTTTGTGCTCGT) of TALEN were designed using online tools (<https://tale-nt.cac.cornell.edu/>) and then generated by FastTALEN Assembly Kit (Sidansai Biotechnology). The plasmids for synthesizing the right and left arms of TALEN were linearized by *NotI* digestion and mRNAs were transcribed in vitro using the mMACHINE SP6 kit (Life Technologies). These mRNAs were purified by the MEGAclean

Transcription Clean-Up Kit (Life Technologies) after adding Poly(A) tail with the Poly(A) Tailing Kit (Life Technologies). Embryos were microinjected together with left and right arm TALEN mRNAs at the one-cell stage. Details of genotyping of embryos are shown in Appendix S1.

2.3 | Generation of transgenic zebrafish

The human *DHX15* and *DHX15* R222G were amplified from the cDNA of the patient's blood sample.⁴ The PCR products were cloned into the modified TOPO vector with heat shock protein 70 promoter.²⁵ The plasmids (25 µg) and Tol2 mRNA transposase (30 µg) were microinjected into one-cell stage embryos to generate *Tg(hsp; DHX15)* and *Tg(hsp; DHX15 R222G)* zebrafish. F0 mosaic embryos were selected by heat shock at 38°C for 1 hour to assess the germline integration of the transgene by checking mCherry fluorescence. F1 zebrafish were generated by intercrossing F0 mosaic adult zebrafish with wildtype zebrafish and confirm germline integration. All the heat-shocked embryos were morphologically normal before undertaking further study.

2.4 | Construction of probe plasmid, synthesis of probe, and WISH

Scl, *cmyb*, *mpx*, *dhx15*, *gata1*, and *hbae1* were cloned from zebrafish cDNA and inserted to pGEM T Easy Vector (Promega) for antisense RNA synthesis. Probe plasmids *lmo2*, *pu.1*, *lyz*, *dab2*, and *ephrinb2* were obtained from Tao Peter Zhong. *Rag1* probe plasmid was a kind gift from Feng Liu. Antisense RNA probes were transcribed in vitro by T3, T7, or Sp6 polymerase (Sigma-Aldrich) with Digoxigenin RNA Labeling Mix (Roche). Primers for probe plasmid construction are listed in Table S1.

WISH was carried out according to the standard protocol.²⁶

2.5 | Whole-mount in situ hybridization

Double immunofluorescence was undertaken using anti-pH3 (Santa Cruz Biotechnology) and anti-GFP Ab (Santa Cruz Biotechnology). *Dhx15*^{+/-}; *Tg(cmyb:gfp)* inbred embryos were fixed overnight in 4% paraformaldehyde and washed with PBST. Embryos were penetrated by 50 µg/ml proteinase K for 15 minutes. After refixation with 4% paraformaldehyde, embryos were washed with PBST, blocked for at least 1 hour with 2% BSA, 10% lamb serum, and 1% Triton-X100 in PBS, and incubated with anti-pH3 (1:200) and anti-GFP (1:200) at 4°C overnight. After being washed with PBST, embryos were incubated with a secondary Ab (1:1000) at 4°C overnight. Embryos were processed for imaging after being washed with PBST.

The TUNEL assay was undertaken with an In Situ Cell Death Detection Kit, TMR red (Roche). Green fluorescent protein immunostaining was carried out as described above.

2.6 | Quantitative RT-PCR and western blot analysis

Embryos generated from *dhx15*^{+/-} were harvested at 2.5-3 dpf. Total RNA was extracted using TRIzol reagent (Sigma-Aldrich) and cDNA were synthesized by using a ReverTra Ace qPCR RT Master Mix with gDNA Remover (Toyobo). Quantitative RT-PCR was carried out using SYBR Premix Ex Taq II (Takara) and run on LightCycler 480 software (Roche). The relative gene expression was quantified as log₂ ratio to β-actin. Higher than 2-fold or lower than 0.5-fold changes of gene expression were considered as significant. Each quantitative PCR experiment was carried out in triplicates. Primers are listed in Table S1.

Protein extracts were resolved on SDS-PAGE gel and transferred to a nitrocellulose membrane, which was probed with Abs against DHX15 (1:1000; Proteintech) or β-actin (1:10 000; CWBIO). After blocking with nonfat milk for 1 hour, the membrane was probed with HRP-conjugated secondary Ab and developed with the Tanon 5200 Chemiluminescent Imaging System (Tanon Science & Technology).

2.7 | Chemical treatment

Dhx15^{+/-} inbred embryos were treated with 4-PBA (50 µM; Sigma-Aldrich) or toyocamycin (100 µM; R&D systems) at 25 hpf, and replaced with fresh 4-PBA or toyocamycin every 24 hpf until the embryos were harvested.

3 | RESULTS

3.1 | Generation of *dhx15*^{-/-} zebrafish

Zebrafish *dhx15* is a highly conserved and maternal gene (Figures S1 and S2). To explore the role of *dhx15* in developmental hematopoiesis, we generated *dhx15*^{-/-} zebrafish by TALEN technology. *Dhx15*^{-/-} zebrafish with a 13 bp deletion in exon 2 were obtained (Figure 1A), which causes early termination at the 129th amino acid (Figure S3). WISH (Figure 1B,B') and western blot analysis (Figure 1C) showed little expression of mRNA or protein in *dhx15*^{-/-} zebrafish. *Dhx15*^{-/-} embryos displayed small eyes, brain necrosis, pericardial edema, and dorsally curved tail (Figure 1D-F,D',F'). These abnormal embryos were genotyped to be *dhx15*^{-/-}, and *dhx15*^{-/-} embryos were distinguished according to the dorsally curved tail after 55 hpf. These embryos are lethal at 5 to 6 dpf.

3.2 | *Dhx15*^{-/-} zebrafish display HSPC failure in CHT

To identify the role of *dhx15* in hematopoiesis, we assessed the status of hematopoietic cell development in *dhx15*^{-/-} embryos. We found expression of *cmyb*, a definitive HSPC marker, was dramatically decreased in CHT at 3 dpf (Figure 2A,A') and 4 dpf (Figure 2B,B'). We

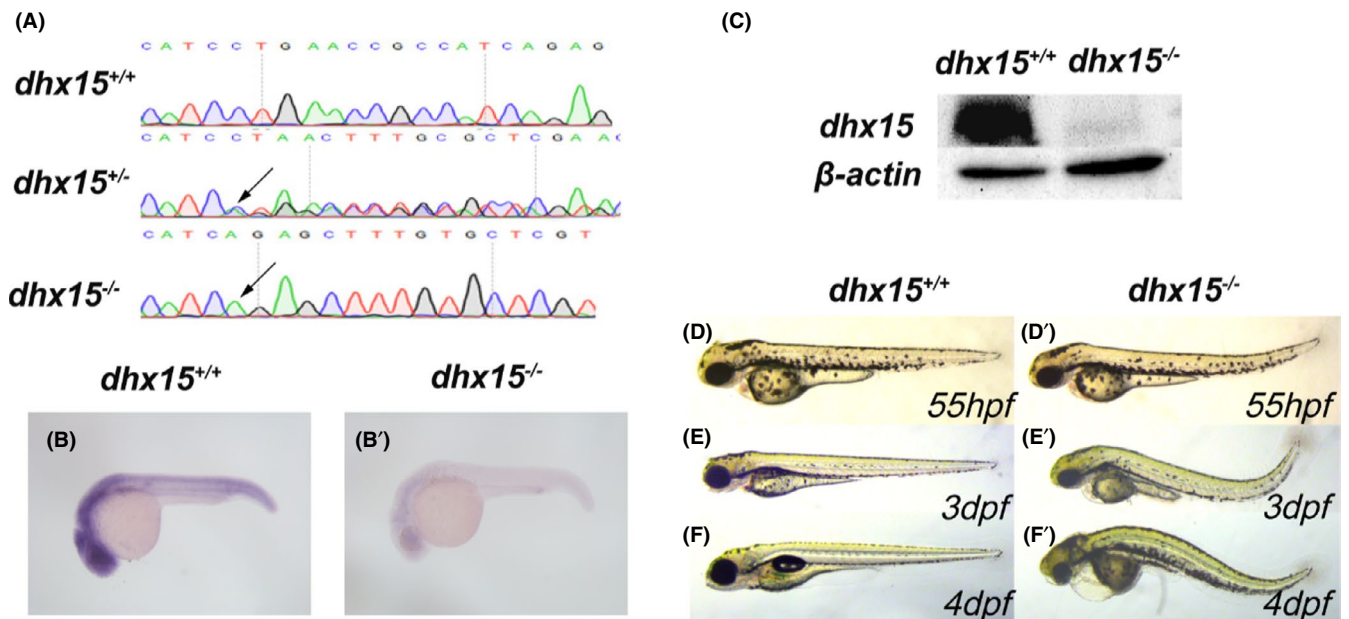


FIGURE 1 Generation of *dhx15*^{-/-} zebrafish. A, DNA sequencing results of *dhx15*^{+/+}, *dhx15*^{+/-}, and *dhx15*^{-/-} embryos. Arrows indicate a 13 bp deletion (CTGAACCGCCATC) at *dhx15* exon 2. B, B', WISH analysis of *dhx15* in *dhx15*^{+/+} and *dhx15*^{-/-} embryos at 24 hpf. C, Western blot analysis of *dhx15* in *dhx15*^{+/+} and *dhx15*^{-/-} embryos at 3 dpf. D-F', Bright-field microscopy images of *dhx15*^{+/+} and *dhx15*^{-/-} zebrafish. dpf, days post fertilization; hpf, hours post fertilization; WISH, whole-mount in situ hybridization

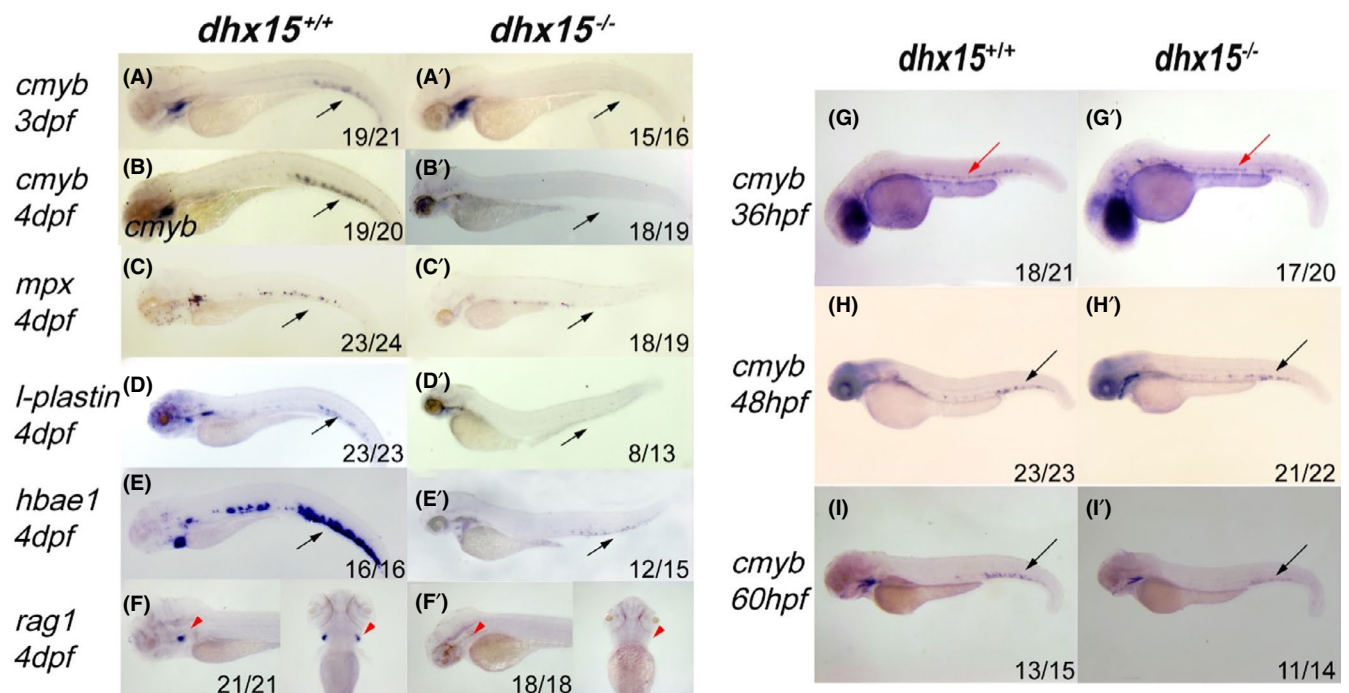


FIGURE 2 *Dhx15*^{-/-} zebrafish displayed defective definitive hematopoiesis in CHT. A-B', WISH analysis of *cmyb* expression in *dhx15*^{+/+} and *dhx15*^{-/-} at 3 dpf (A, A') and 4 dpf (B, B'). C-F', WISH analysis of *mpx* (C, C'), *l-plastin* (D, D'), *hbae1* (E, E'), *rag1* (F, F') expression in *dhx15*^{+/+} and *dhx15*^{-/-} zebrafish. G-I', WISH analysis of *cmyb* expression in *dhx15*^{+/+} and *dhx15*^{-/-} zebrafish at 36 hpf (G, G'), 48 hpf (H, H'), 60 hpf (I, I'). Black arrows indicate CHT; red arrows indicate ventral wall of dorsal aorta; red arrowheads indicate thymus. CHT, caudal hematopoietic tissue; dpf, days post fertilization; hpf, hours post fertilization; WISH, whole-mount in situ hybridization

further examined expression of the downstream hematopoietic cell markers in *dhx15*^{-/-} embryos: *mpx* (neutrophil marker) (Figure 2C,C'), *l-plastin* (pan-myeloid cell marker) (Figure 2D,D'), *hbae1* (erythrocyte marker) (Figure 2E,E'), and *rag1* (lymphocyte marker) (Figure 2F,F').

These mature definitive hematopoietic cells displayed a remarkable decrease in CHT, indicating that *dhx15*^{-/-} zebrafish experienced severe mature definitive defects. The HSPC failure in *dhx15* knockout embryos were further confirmed by CD41^{low} HSPCs in

the *Tg(CD41:gfp)* zebrafish²⁷ (Figure S4). These data suggested that *dhx15* knockout results in HSPC failure in zebrafish, and the HSPC failure does not originate from accelerated differentiation of matured hematopoietic cells.

We also assessed primitive hematopoiesis in *dhx15*^{-/-} embryos. The expression of *scl* (stem cell marker) (Figure S5A,A'), *gata1* (erythrocyte progenitor cell marker) (Figure S5B,B'), *band3* (hemoglobin marker) (Figure S5C,C'), and *l-plastin* (Figure S5D,D') was normal when *dhx15* was absent, indicating primary hematopoiesis is not affected in *dhx15*^{-/-} embryos.

To our knowledge, zebrafish definitive hematopoiesis initiates in the VDA, migrates to CHT, and undergoes expansion and differentiation in CHT. To further investigate when the HSPC failure initiates, we undertook a time course WISH analysis of *cmyb* from 36 hpf to 60 hpf. The expression of *cmyb* in the VDA at 36 hpf (Figure 2G,G') and CHT at 48 hpf (Figure 2H,H') were unaffected. In contrast, a marginal decrease of *cmyb* expression was observed in CHT at 60 hpf (Figure 2I,I'). These results indicated that HSPCs initiate in the VDA, and could migrate from the VDA to CHT in *dhx15*^{-/-} embryos. However, HSPCs are severely affected in CHT after 48 hpf.

Vascular development²⁸ and blood flow²⁹ are known prerequisites for HSPC development. In *Tg(dhx15*^{-/-}; *flk:egfp*) embryos, expression of *flk* (endothelial cell marker) is normal compared to wildtype siblings (Figure S6A,A'). The WISH analysis showed that *ephrinb2* (arterial endothelial marker) and *dab2* (venous endothelial marker) were unaffected in *dhx15*^{-/-} zebrafish (Figure S6B,C, B',C'). Furthermore, visual inspection of blood flow by bright-field microscopy showed no difference between *dhx15*^{-/-} embryos and wildtype sibling embryos at 3 dpf (data not shown). According to these results, HSPC failure observed in *dhx15*^{-/-} embryos was not secondary to aberrant vascular development or blood flow.

McElderry et al³⁰ undertook a similar analysis and attributed HSPC failure to the secondary effects of morphological phenotypes in *dhx15*^{-/-} embryos. However, we utilized *dhx15* morpholino to knockdown *dhx15* and found impaired primary hematopoiesis and HSPC failure (Figure S7), indicating that *dhx15* plays an important role in zebrafish hematopoiesis, and the HSPC failure is not a secondary effect of morphological phenotype.

3.3 | Abated proliferation but not excessive apoptosis of HSPCs is observed in *dhx15*^{-/-} zebrafish

To determine how HSPCs in *dhx15*^{-/-} zebrafish were disturbed, TUNEL assay analysis was applied. The apoptotic HSPCs in CHT were analysed (Figure 3A). We found that *dhx15*^{-/-} zebrafish showed comparable apoptotic signals in CHT to wildtype zebrafish at 48 hpf (Figure 3B,F; wildtype, 1.2 ± 0.2494 , $n = 10$; *dhx15*^{-/-}, 1.25 ± 0.1637 , $n = 8$; $P > .05$, Student's *t* test). Although significantly increased apoptotic signals in CHT were detected in *dhx15*^{-/-} zebrafish at 60 hpf (Figure 3C,F; wildtype, 2.063 ± 0.3923 , $n = 16$; *dhx15*^{-/-}, 10.91 ± 1.944 , $n = 11$; $P < .005$, Student's *t* test), the apoptotic

signal could be hardly observed in HSPCs (Figure 3C,G; wildtype, 0.125 ± 0.08539 , $n = 16$; *dhx15*^{-/-}, 0.1818 ± 0.122 , $n = 11$; $P > .05$, Student's *t* test). It is known that the p53 pathway plays an important role in the regulation of cell proliferation and apoptosis.³¹ The study by McElderry et al³⁰ reported increased p53 expression in *dhx15*^{-/-} zebrafish. However, our WISH analysis showed minimal effects in reverting HSPC failure by knocking down p53 using p53 morpholino (Figure S8). Taken together, we reasoned that HSPC failure in CHT was p53-independent and not resulting from excessive apoptosis.

Double immunofluorescence staining with GFP and pH3 was carried out in *dhx15*^{-/-}; *Tg(cmyb:gfp)* and *dhx15*^{+/+}; *Tg(cmyb:gfp)* zebrafish to study the proliferating status of HSPCs. PH3-positive HSPCs were markedly reduced in *dhx15*^{-/-} zebrafish compared with wildtype embryos at 60 hpf (Figure 3E,H; wildtype, 7.464 ± 0.9413 , $n = 11$; *dhx15*^{-/-}, 2.367 ± 0.6178 , $n = 9$; $P < .005$, Student's *t* test), whereas the number of pH3-positive HSPCs was not altered in *dhx15*^{-/-} zebrafish at 48 hpf (Figure 3D; wildtype, 11.34 ± 2.379 , $n = 9$; *dhx15*^{-/-}, 13.98 ± 1.829 , $n = 11$; $P > .05$, Student's *t* test). These results indicated that the HSPC failure is a result of decreased HSPC proliferation.

3.4 | Unfolded protein response pathway mediates HSPC failure in *dhx15*^{-/-} zebrafish

A study has reported differential expression of splicing genes and alternative events following the loss of DHX15,⁷ which would increase protein variants. These abnormal proteins might not proceed normal protein synthesis and give rise to increased ER stress (UPR). ER regulation is critical in different states of HSC and governs the integrity of the HSC pool.³²

To further investigate whether *dhx15* deletion results in UPR-mediated HSPC failure in *dhx15*^{-/-} embryos, qRT-PCR was used (Figure S9). We found that the expression of UPR-related genes *CHOP*, *ATF3*, and *JUN* were dramatically increased in *dhx15*^{-/-} zebrafish (Figure 4A). *CHOP* and *ATF3* play important roles in the UPR pathway (reviewed in Schroder et al,³⁷) and *JUN* is an upstream factor regulating UPR in AML.⁴⁰ We used 4-PBA, a UPR small molecule inhibitor, which enhances protein folding to suppress the increase of ER stress.³³ The WISH analysis showed *dhx15*^{-/-} HSPC failure could be partially rescued in *dhx15*^{-/-} zebrafish treated with 4-PBA (Figure 4B-E; $P < .005$, χ^2 test). There are three arms of UPR pathway: IRE1-XBP1, ATF6, and PERK.³⁴ We used Toyocamycin, a small molecule inhibitor of ER stress-induced XBP1 mRNA splicing, to suppress UPR.³⁵ Results showed that *dhx15*^{-/-} HSPC failure could be partially rescued in *dhx15*^{-/-} zebrafish treated with toyocamycin (Figure 4F-I; $P < .005$, χ^2 test). Salubrinal, another UPR inhibitor that targets at the PERK arm,³⁶ was used to rescue the HSPC failure, but no significant difference was observed (Table S2). These data suggest that HSPC failure is mediated, in part, through the UPR pathway.

To mimic the overexpressed DHX15 in AML patients and study the function of the DHX15/DHX15 R222G, we generated *Tg(hsp: DHX15)* and *Tg(hsp: DHX15 R222G)* transgenic zebrafish

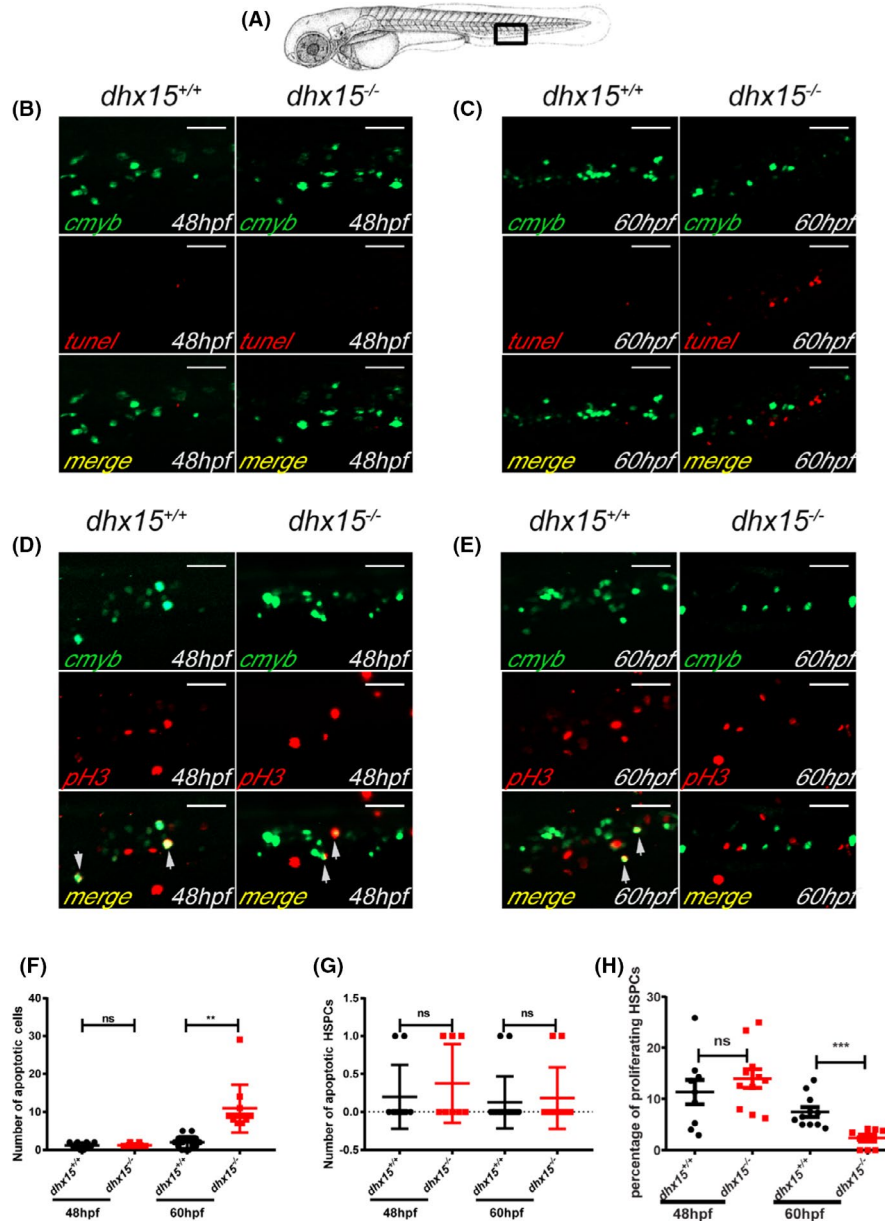


FIGURE 3 Abated proliferation but not excessive apoptosis of HSPCs is observed in *dhx15*^{-/-} zebrafish. A, Schematic indicates the area of the imaging in the tail (CHT), outlined by the black box. B, C, Fluorescence images of the *cmyb* and apoptotic cells in CHT of *dhx15*^{+/+}; *Tg(cmyb:gfp)* and *dhx15*^{-/-}; *Tg(cmyb:gfp)* zebrafish embryos at 48 hours post fertilization (hpf) (B) and 60 hpf (C). D, E, Fluorescence images of pH3 and *cmyb* positive cells in CHT of *dhx15*^{+/+}; *Tg(cmyb:gfp)* and *dhx15*^{-/-}; *Tg(cmyb:gfp)* zebrafish embryos at 48 hpf (D) and 60 hpf (E). F, Number of apoptotic cells in CHT at 48 hpf (wildtype, 1.2 ± 0.2494 , $n = 10$; *dhx15*^{-/-} embryos, 1.25 ± 0.1637 , $n = 8$; $P > .05$, Student's *t* test) and 60 hpf (wildtype, 2.063 ± 0.3923 , $n = 16$; *dhx15*^{-/-} embryos, 10.91 ± 1.944 , $n = 11$; $P < .005$, Student's *t* test). G, Number of apoptotic HSPCs in CHT at 48 hpf (wildtype, 0.2 ± 0.1333 , $n = 10$; *dhx15*^{-/-} embryos, 0.375 ± 0.183 , $n = 8$; $P > .05$, Student's *t* test) and 60 hpf (wildtype, 0.125 ± 0.08539 , $n = 16$; *dhx15*^{-/-} embryos, 0.1818 ± 0.122 , $n = 11$; $P > .05$, Student's *t* test). H, Percentages of proliferating HSPCs in CHT at 48 hpf (wildtype, 11.34 ± 2.379 , $n = 9$; *dhx15*^{-/-} embryos, 13.98 ± 1.829 , $n = 11$; $P > .05$, Student's *t* test) and 60 hpf (wildtype, 7.464 ± 0.9413 , $n = 11$; *dhx15*^{-/-} embryos, 2.367 ± 0.6178 , $n = 9$; $P < .0005$, Student's *t* test). Data are represented as mean \pm SEM. * $P < .05$; ** $P < .005$; *** $P < .0005$. Scale bar = 40 μ m. CHT, caudal hematopoietic tissue; hpf, hours post fertilization; HSPCs, hematopoietic stem/progenitor cells; ns, not significant; pH3, pospho-histone H3

that ectopically overexpress DHX15 and DHX15 R222G under heat activation. DHX15 and DHX15 R222G expression were confirmed by mCherry fluorescence under a fluorescence microscope (Figure S10). The embryos were morphologically normal after heat treatment. The mCherry fluorescence-positive embryos were

selected for further study. The WISH analysis showed expression of definitive hematopoietic markers *cmyb* (Figure 5A,A',A''), *hbae1* (Figure 5B,B',B''), *mpx* (Figure 5C,C',C''), and *rag1* (Figure 5D,D',D'') are unaffected in both *Tg(hsp: DHX15)* and *Tg(hsp: DHX15 R222G)* transgenic zebrafish.

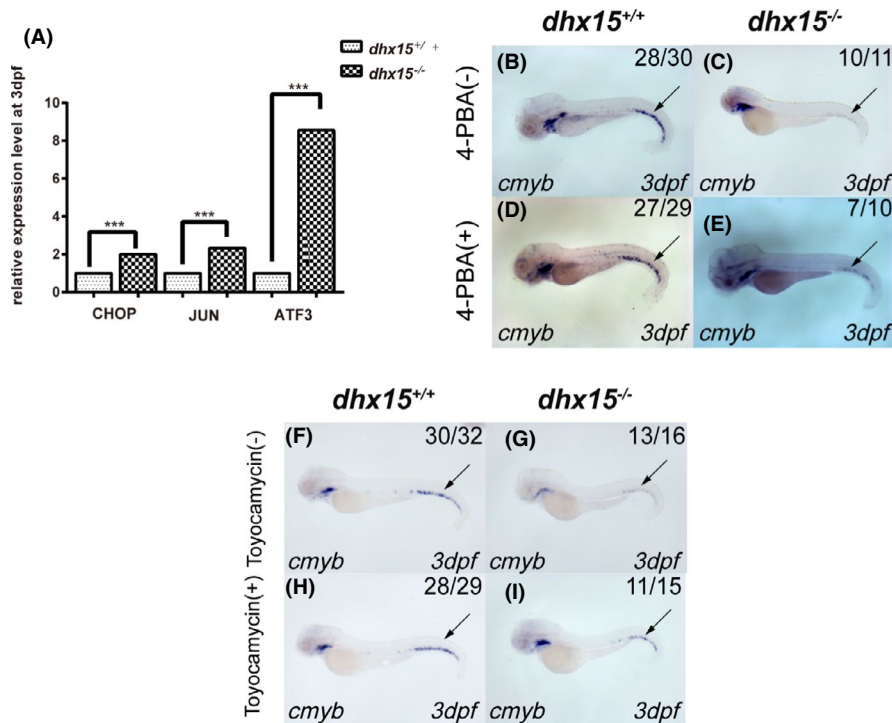


FIGURE 4 UPR pathway mediates HSPC failure in *dhx15*^{-/-} zebrafish. A, qRT-PCR analysis of CHOP, JUN, and ATF3 in *dhx15*^{+/+} and *dhx15*^{-/-} zebrafish at 3 dpf. Each qRT-PCR experiment was carried out in triplicates, and repeated at least three times. B-E, WISH analysis of *cmyb* in *dhx15*^{+/+} and *dhx15*^{-/-} zebrafish treated with 4-PBA. $P < .005$, χ^2 test. F-I, WISH analysis of *cmyb* in *dhx15*^{+/+} and *dhx15*^{-/-} zebrafish treated with toyocamycin. $P < .005$, χ^2 test. Black arrow indicates caudal hematopoietic tissue. *** $P < .0005$. ATF3, activating transcription factor 3; dpf, days post fertilization; HSPC, hematopoietic stem/progenitor cell; qRT-PCR, quantitative real-time PCR; UPR, unfolded protein response pathway; WISH, whole-mount in situ hybridization; 4-PBA, 4-phenylbutyric acid

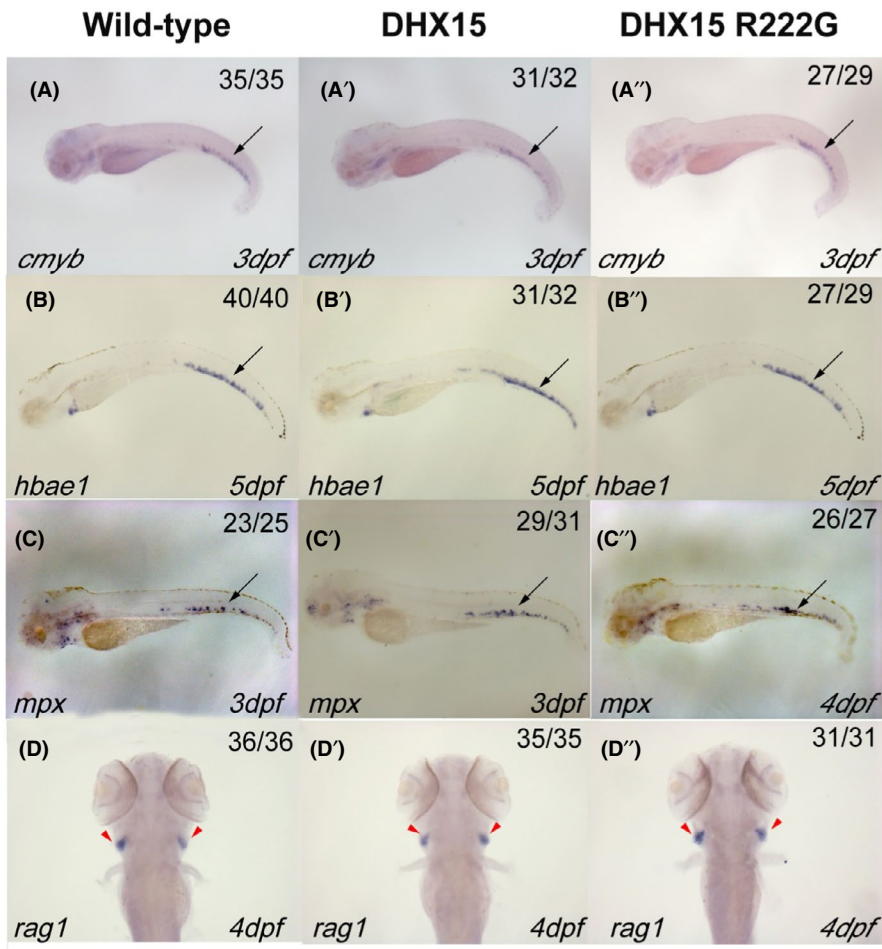


FIGURE 5 Definitive hematopoiesis in zebrafish is normal when DHX15 or DHX15 R222G is overexpressed. WISH analysis of definitive hematopoietic markers: *cmyb* (A-A''), *hbae1* (B-B''), *mpx* (C-C''), and *rag1* (D-D''). Embryos from wildtype, *Tg(hsp: DHX15)*, and *Tg(hsp: DHX15 R222G)* zebrafish were heat-shocked at 38°C for 2 h every day since 25 hours post fertilization (hpf). DHX15, *Tg(hsp: DHX15)*; DHX15 R222G, *Tg(hsp: DHX15 R222G)*. Black arrows indicate caudal hematopoietic tissue; red arrowheads indicate thymus. hpf, hours post fertilization; WISH, whole-mount in situ hybridization

3.5 | Role of DHX15 R222G in zebrafish hematopoiesis

Many studies have reported the DHX15 R222G mutation in AML patients,^{5,7,8,9} but the function of the mutation in hematopoiesis remains elusive. We obtained *dhx15^{+/-}; Tg(hsp: DHX15)* and *dhx15^{+/-}; Tg(hsp: DHX15 R222G)* by crossing *Tg(hsp: DHX15)* and *Tg(hsp: DHX15 R222G)* with *dhx15^{+/-}*, respectively. Then we inbred *dhx15^{+/-}; Tg(hsp: DHX15)* or *dhx15^{+/-}; Tg(hsp: DHX15 R222G)* and the embryos were subjected to 38°C for 1 hour and 45 minutes every day after 25 hpf. The mCherry fluorescence-positive embryos were selected for

further study. Embryos were also harvested for western blot analysis (Figure 6). Both DHX15 or DHX15 R222G overexpression restored HSPC failure in *dhx15^{-/-}* zebrafish (Figure 6B',C' and Table 1). However, DHX15 R222G is not as effective as DHX15 in restoring HSPC failure (Figure 6 and Table 1; DHX15 HS vs DHX15 R222G HS, $P < .05$, χ^2 test). We prolonged the heat-shock time to 2 hours to increase the expression level of DHX15 R222G (Figure 6D), but there was no significant difference between DHX15 and DHX15 R222G groups (Figure 6B',C'' and Table 1; $P > .05$, χ^2 test). These data suggest that the function of DHX15 in zebrafish hematopoiesis is compromised after R222G mutation.

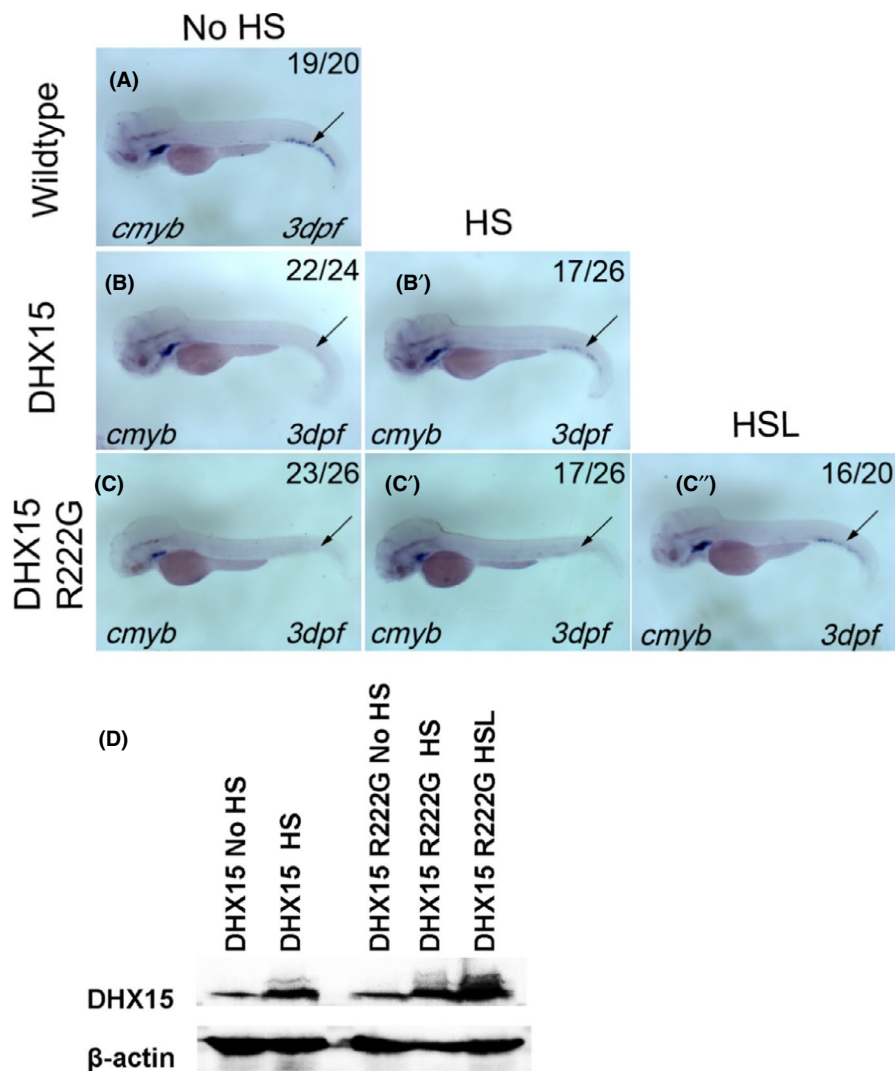


FIGURE 6 DHX15 R222G is not as effective as DHX15 in restoring HSPC failure in *dhx15^{-/-}* zebrafish. A, *cmyb* expression of wildtype zebrafish at 3 dpf. B, B', *cmyb* expression of *Dhx15^{-/-}; Tg(hsp: DHX15)* zebrafish at 3 dpf with (B') or without (B) heat-shock treatment. HSPC failure was rescued after DHX15 overexpression in *dhx15^{-/-}* zebrafish ($P < .0001$, χ^2 test). C-C'', *cmyb* expression of *Dhx15^{-/-}; Tg(hsp: DHX15 R222G)* zebrafish at 3 dpf with (C', C'') or without (C) HS treatment. HSPC failure was rescued after DHX15 R222G overexpression in *dhx15^{-/-}* zebrafish ($P < .05$, χ^2 test). DHX15 R222G is not as effective as DHX15 in restoring HSPC failure in *dhx15^{-/-}* zebrafish. (No HS vs HS, $P < .05$, χ^2 test; No HS vs HSL, $P < .0001$, χ^2 test; HS vs HSL, $P < .005$, χ^2 test). D, Western blot analysis of DHX15 protein expression in DHX15/DHX15 R222G transgenic zebrafish with or without heat activation. DHX15, *Dhx15^{-/-}; Tg(hsp: DHX15)*; DHX15 R222G, *Dhx15^{-/-}; Tg(hsp: DHX15 R222G)*; dpf, days post fertilization; hpf, hours post fertilization; HS, heat-shocked at 38°C for 1 h and 45 min once a day since 25 hpf; HSL, heat-shocked at 38°C for 2 h once a day since 25 hpf; HSPC, hematopoietic stem/progenitor cell; No HS, without heat-shock treatment. Black arrow indicates caudal hematopoietic tissue

DHX15 No HS vs DHX15 HS	$P < .0001^{****}$
DHX15 R222G No HS vs DHX15 R222G HS	$P < .05^*$
DHX15 R222G No HS vs DHX15 R222G HSL	$P < .0001^{****}$
DHX15 HS vs DHX15 R222G HS	$P < .05^*$
DHX15 R222G HS vs DHX15 R222G HSL	$P < .005^{**}$
DHX15 HS vs DHX15 R222G HSL	$P > .05$ ns

Abbreviations: HS, heat-shocked at 38°C for 1 h and 45 min once a day since 25 hpf; HSL, heat-shocked at 38°C for 2 hours once a day since 25 hpf; HSPC, hematopoietic stem/progenitor cell; No HS, without heat-shock treatment; ns, not significant.

* $P < .05$; ** $P < .005$; **** $P < .0001$.

TABLE 1 Statistical analysis of rescuing the HSPC failure in *dhx15*^{-/-} zebrafish overexpressed DHX15/DHX15 R222G

4 | DISCUSSION

Previously, we found that DHX15 is upregulated in AML patients and is associated with poor prognosis.⁴ *Dhx15*^{-/-} zebrafish was generated to further study the role of *dhx15* in developmental hematopoiesis. In the *dhx15*^{-/-} zebrafish, primary hematopoiesis is normal, but definitive hematopoiesis is severely disturbed. McElderry et al³⁰ attributed hematopoietic failure in their *dhx15* knockout zebrafish to pleiotropic morphological defects. Here, we utilized *dhx15* morpholino to knock down *dhx15* and found definitive hematopoietic failure at 3 dpf. These embryos showed normal morphological development, indicating that *dhx15* is critical in definitive hematopoiesis and is independent of morphological defects. We found primary hematopoiesis is impaired when *dhx15* is knocked down, whereas *dhx15* knockout zebrafish showed normal primary hematopoiesis. This might be due to the maternal transcript of *dhx15* during early embryonic development. Taken together, the results suggested that *dhx15* is critical in zebrafish hematopoiesis, and is independent of morphological defects.

The migration of HSPCs from the VDA to CHT initiates at approximately 48 hpf, and continues after 48 hpf.²² We detected normal expression of HSPCs in CHT at 48 hpf, and a marginal decrease at 60 hpf. The HSPC failure might be due to a migration defect from the VDA and CHT after 48 hpf. As the HSPC failure is observed when the dorsally curved tail is present, it is also possible that the HSPC failure is a result of impaired HSPC maintenance in CHT (affected by the curved tail), which the HSPCs seed to CHT, but are not able to expand and differentiate.

UPR is a cellular response triggered by accumulation of unfolded protein in the ER. Activation of UPR aims at restoring ER stress, but cells could undergo apoptosis when the ER is overloaded (reviewed in Schroder et al³⁷). It has been reported that ER regulation is critical in different states of HSC (reviewed in Boyce et al³⁸) and governs the integrity of the hematopoietic stem cell pool.³² Sigurdsson et al³⁹ reported that the number of bone marrow HSCs significantly decreased when ER stress was elevated, indicating that a proper level of ER stress is important in the developmental stage of HSCs. In *dhx15*^{-/-} zebrafish, we found that the UPR pathway-related molecules CHOP, ATF3, and JUN^{37,40} are upregulated, and the UPR small molecular inhibitor 4-PBA and toyocamycin could rescue HSPC failure. The inhibition of the IRE1-XBP1 arm (toyocamycin) could rescue HSPC failure in *dhx15* knockout embryos, indicating that the HSPC

failure is mediated, at least in part, through the IRE1-XBP1 arm of UPR. However, we did not observe increased IRE1a or XBP1 expression in *dhx15* knockout embryos through qTR-PCR. It is possible that the function of the molecules in the UPR pathway function through different format, for example: trans-autophosphorylation of IRE1; spliced and unspliced XBP1. So, it might not show differences in RNA or protein expression level.

Although the activated UPR pathway is well recognized to trigger cell apoptosis (reviewed in Schroder et al³⁷), our data showed decreased proliferation instead of increased apoptosis of HSPCs in *dhx15*^{-/-} zebrafish. Some studies have shown UPR pathway-mediated inhibition of cell proliferation.^{41,42} We proposed that upregulated ER stress and activation of the UPR pathway in *dhx15*^{-/-} zebrafish might inhibit the proliferation of HSPCs, resulting in HSPC failure. Another possibility is that UPR in nonhematopoietic cells contributes to the HSPC failure. The zebrafish complex CHT niche contains multiple cell types, including stromal cells, vascular endothelial cells, and hematopoietic cells. The microenvironment of the CHT niche is critical for HSPC maintenance.⁴³ Our data showed increased apoptotic cells in CHT in *dhx15* knockout embryos, but these apoptotic cells are not HSPCs (Figure 3F,G). It is possible that increased ER stress leads to nonhematopoietic cell apoptosis. The loss of nonhematopoietic cells in CHT would not be able to support HSPC survival in CHT. But the specific mechanism warrants further study.

In this study, we generated transgenic zebrafish that overexpressed DHX15 to mimic upregulated DHX15 status in AML patients. The definitive hematopoiesis remains unaffected when DHX15 is dramatically overexpressed. The discrepancy could be due to one of the following factors: (a) DHX15 normally functions by interacting with other proteins,^{15,44} only co-overexpress with these proteins could display the related phenotypes in zebrafish; (b) DHX15 expression is not enough to reach the threshold of disrupting hemostasis in hematopoiesis; and (c) Genetic background has more profound effects on gene overexpression phenotypes in AML patients compared with zebrafish.

The function of DHX15 R222G in vivo was studied. We found compromised DHX15 R222G function in restoring HSPC failure in *dhx15*^{-/-} zebrafish compared with DHX15. It has been reported that impaired pre-mRNA splicing when DHX15 R222G were overexpressed in vitro, and decreased DHX15 R222G-TFIP11 interaction compared with DHX15-TFIP11 interaction.⁷ We reasoned that DHX15 R222G

might act as a loss of function in developmental hematopoiesis. Thus, DHX15 R222G could not reach the same efficacy in restoring HSPC failure as DHX15. However, it might be another story in AML patients with DHX15 R222G. Studies have reported DHX15 R222G in both de novo and relapsed AML patients,^{7,8} and this mutation disappeared when the patients achieved remission.^{4,8} We found the peripheral blood blasts of AML patients with R222G mutation is higher than in those without mutation (Tables S3 and S4). The median overall survival tends to be higher, and the complete remission rate after one and two courses of chemotherapy tend to be lower in AML patients without the mutation (Figure S11). These results suggest DHX15 R222G might serve as an indicator in AML development. Increased alternative splicing has been reported when DHX15 R222G is overexpressed in vitro.⁷ We hypothesize that, in AML patients with DHX15 R222G, increased alternative splicing events result in differential gene variants. These variant alterations could result in impaired HSPC differentiation. This might explain the higher percentage of peripheral blood blasts and poorer outcomes in AML patients with DHX15 R222G. More patients with DHX15 R222G are needed to add to the group to further elucidate the role of DHX15 R222G in AML pathogenesis.

Here, we provide new insights into the role of *dhx15* and the DHX15 R222G mutation in zebrafish hematopoiesis. *Dhx15* regulates zebrafish definitive hematopoiesis through the UPR pathway. We revealed compromised function in definitive hematopoiesis of DHX15 R222G in *dhx15*^{-/-} zebrafish. These results indicate that *dhx15* is an important regulator in zebrafish definitive hematopoiesis. The role of *dhx15* and DHX15 R222G in developmental hematopoiesis could provide new insight into DHX15 upregulated/DHX15 R222G AML development.

ACKNOWLEDGMENTS

We appreciate all the members in Tao Peter Zhong's laboratory for technical support and helpful discussions. We thank Feng Liu for the *rag1* probe for WISH. This work was supported by: National Natural Science Foundation of China, Grant/Award Numbers: 81770163, 81270609, 81470008, 81500139; Fujian Province Health Education Joint Research Project, Grant/Award Number: WKJ-2016-2-07; Special Funding of Fujian Provincial Department of Finance, Grant/Award Number: Min2017-655; Construction Project of Fujian Medical Center of Hematology, Grant/Award Number: Min201704; The National and Fujian Provincial Key Clinical Specialty Discipline Construction Program, PRC, Grant/Award Number: 2011-1006, 2012-149.

CONFLICT OF INTEREST

The authors have no conflict of interest.

ORCID

Shaoyuan Wang  <https://orcid.org/0000-0001-7428-8682>

REFERENCES

- Bolli N, Payne EM, Grabher C, et al. Expression of the cytoplasmic NPM1 mutant (NPMc+) causes the expansion of hematopoietic cells in zebrafish. *Blood*. 2010;115(16):3329-3340.
- He B-L, Shi X, Man CH, et al. Functions of *flt3* in zebrafish hematopoiesis and its relevance to human acute myeloid leukemia. *Blood*. 2014;123(16):2518-2529.
- Shi X, He B-L, Ma ACH, et al. Functions of *idh1* and its mutation in the regulation of developmental hematopoiesis in zebrafish. *Blood*. 2015;125(19):2974-2984.
- Pan L, Li Y, Zhang H, et al. DHX15 is associated with poor prognosis in acute myeloid leukemia (AML) and regulates cell apoptosis via the NF- κ B signaling pathway. *Oncotarget*. 2017;8(52):89643-89654.
- Madan V, Han L, Hattori N, et al. ASXL2 regulates hematopoiesis in mice and its deficiency promotes myeloid expansion. *Haematologica*. 2018;103(12):1980-1990.
- Christen F, Hoyer K, Yoshida K, et al. Genomic landscape and clonal evolution of acute myeloid leukemia with t(8; 21): an international study on 331 patients. *Blood*. 2019;133(10):1140-1151.
- Faber ZJ, Chen X, Gedman AL, et al. The genomic landscape of core-binding factor acute myeloid leukemias. *Nat Genet*. 2016;48(12):1551-1556.
- Farrar JE, Schuback HL, Ries RE, et al. Genomic Profiling of Pediatric Acute Myeloid Leukemia Reveals a Changing Mutational Landscape from Disease Diagnosis to Relapse. *Can Res*. 2016;76(8):2197-2205.
- Sood R, Hansen NF, Donovan FX, et al. Somatic mutational landscape of AML with *inv(16)* or *t(8;21)* identifies patterns of clonal evolution in relapse leukemia. *Leukemia*. 2016;30(2):501-504.
- Taskesen E, Havermans M, Kv L, et al. Two splice-factor mutant leukemia subgroups uncovered at the boundaries of MDS and AML using combined gene expression and DNA-methylation profiling. *Blood*. 2014;123(21):3327-3335.
- Martin A, Schneider S, Schwer B. Prp43 Is an Essential RNA-dependent ATPase Required for Release of Lariat-Intron from the Spliceosome. *J Biol Chem*. 2002;277(20):17743-17750.
- Memet I, Doebele C, Sloan KE, Bohnsack MT. The G-patch protein NF- κ B-repressing factor mediates the recruitment of the exonuclease XRN2 and activation of the RNA helicase DHX15 in human ribosome biogenesis. *Nucleic Acids Res*. 2017;gkx013. <https://doi.org/10.1093/nar/gkx013>
- Lebaron S, Papin C, Capeyrou R, et al. The ATPase and helicase activities of Prp43p are stimulated by the G-patch protein Pfa1p during yeast ribosome biogenesis. *EMBO J*. 2009;28(24):3808-3819. <https://doi.org/10.1038/emboj.2009.335>
- Lin M-L, Fukukawa C, Park J-H, et al. Involvement of G-patch domain containing 2 overexpression in breast carcinogenesis. *Cancer Sci*. 2009;100(8):1443-1450.
- Jing Y, Nguyen MM, Wang D, et al. DHX15 promotes prostate cancer progression by stimulating Siah2-mediated ubiquitination of androgen receptor. *Oncogene*. 2018;37(5):638-650.
- Xie C, Liao H, Zhang C, Zhang S. Overexpression and clinical relevance of the RNA helicase DHX15 in hepatocellular carcinoma. *Hum Pathol*. 2019;84:213-220.
- Xu Y, Song Q, Pascal LE, et al. DHX15 is up-regulated in castration-resistant prostate cancer and required for androgen receptor sensitivity to low DHT concentrations. *Prostate*. 2019;79(6):657-666.
- Chen AT, Zon LI. Zebrafish blood stem cells. *J Cell Biochem*. 2009;108(1):35-42.
- Bertrand JY, Kim AD, Teng S, Traver D. CD41+ *cmyb*+ precursors colonize the zebrafish pronephros by a novel migration route to initiate adult hematopoiesis. *Development*. 2008;135(10):1853-1862.
- Burns CE, DeBlasio T, Zhou Y, Zhang J, Zon L, Nimer SD. Isolation and characterization of *runxa* and *runxb*, zebrafish members of the runt family of transcriptional regulators. *Exp Hematol*. 2002;30(12):1381-1389.
- Jin H, Xu J, Wen Z. Migratory path of definitive hematopoietic stem/progenitor cells during zebrafish development. *Blood*. 2007;109(12):5208-5214.

22. Murayama E, Kissa K, Zapata A, et al. Tracing Hematopoietic Precursor Migration to Successive Hematopoietic Organs during Zebrafish Development. *Immunity*. 2006;25(6):963-975.
23. North TE, Goessling W, Walkley CR, et al. Prostaglandin E2 regulates vertebrate haematopoietic stem cell homeostasis. *Nature*. 2007;447(7147):1007.
24. Jin S-W, Beis D, Mitchell T, Chen J-N, Stainier DY. Cellular and molecular analyses of vascular tube and lumen formation in zebrafish. *Development*. 2005;132(23):5199-5209.
25. Jin D, Zhu D, Fang Y, et al. Vegfa signaling regulates diverse artery/vein formation in vertebrate vasculatures. *J Genet Genom*. 2017;44(10):483-492.
26. Thisse C, Thisse B. High-resolution in situ hybridization to whole-mount zebrafish embryos. *Nat Protoc*. 2008;3(1):59-69.
27. Ma D, Zhang J, Hf L, Italiano J, Handin RI. The identification and characterization of zebrafish hematopoietic stem cells. *Blood*. 2011;118(2):289-297.
28. Adamo L, Garcia-Cardena G. The vascular origin of hematopoietic cells. *Dev Biol*. 2012;362(1):1-10.
29. North TE, Goessling W, Peeters M, et al. Hematopoietic stem cell development is dependent on blood flow. *Cell*. 2009;137(4):736-748.
30. McElderry J, Carrington B, Bishop K, et al. Splicing factor DHX15 affects tp53 and mdm2 expression via alternate splicing and promoter usage. *Hum Mol Genet*. 2019;28(24):4173-4185.
31. Symonds H, Krall L, Remington L, et al. p53-dependent apoptosis suppresses tumor growth and progression in vivo. *Cell*. 1994;78(4):703-711.
32. van Galen P, Kreso A, Mbong N, et al. The unfolded protein response governs integrity of the haematopoietic stem-cell pool during stress. *Nature*. 2014;510(7504):268-272.
33. Murayama E, Sarris M, Redd M, et al. NACA deficiency reveals the crucial role of somite-derived stromal cells in haematopoietic niche formation. *Nat Commun*. 2015;6:8375.
34. Ron D, Walter P. Signal integration in the endoplasmic reticulum unfolded protein response. *Nat Rev Mol Cell Biol*. 2007;8(7):519-529.
35. Ri M, Tashiro E, Oikawa D, Shinjo S, Tokuda M, Yokouchi Y, et al. Identification of Toyocamycin, an agent cytotoxic for multiple myeloma cells, as a potent inhibitor of ER stress-induced XBP1 mRNA splicing. *Blood Cancer J*. 2012;2(7):e79.
36. Boyce M, Bryant KF, Jousse C, et al. A Selective Inhibitor of eIF2 α Dephosphorylation Protects Cells from ER. *Stress*. 2005;307(5711):935-939.
37. Schroder M, Kaufman RJ. The mammalian unfolded protein response. *Annu Rev Biochem*. 2005;74:739-789.
38. Sigurdsson V, Miharada K. Regulation of unfolded protein response in hematopoietic stem cells. *Int J Hematol*. 2018;107(6):627-633.
39. Sigurdsson V, Takei H, Soboleva S, et al. Bile Acids Protect Expanding Hematopoietic Stem Cells from Unfolded Protein Stress in Fetal Liver. *Cell Stem Cell*. 2016;18(4):522-532.
40. Zhou C, Martinez E, Di Marcantonio D, et al. JUN is a key transcriptional regulator of the unfolded protein response in acute myeloid leukemia. *Leukemia*. 2017;31(5):1196-1205.
41. Liu B-Q, Gao Y-Y, Niu X-F, et al. Implication of unfolded protein response in resveratrol-induced inhibition of K562 cell proliferation. *Biochem Biophys Res Comm*. 2010;391(1):778-782.
42. Fan LX, Liu CM, Gao AH, Zhou YB, Li J. Berberine combined with 2-deoxy-d-glucose synergistically enhances cancer cell proliferation inhibition via energy depletion and unfolded protein response disruption. *Biochem Biophys Acta*. 2013;1830(11):5175-5183.
43. Nik S, Weinreb JT, Bowman TV. Developmental HSC Microenvironments: Lessons from Zebrafish. *Adv Exp Med Biol*. 2017;1041:33-53.
44. Arenas JE, Abelson JN. Prp43₃ An RNA helicase-like factor involved in spliceosome disassembly. *Biochemistry*. 1997;94:11798-11802.

SUPPORTING INFORMATION

Additional supporting information may be found online in the Supporting Information section.

How to cite this article: Cai Y, Wang J, Jin D, et al. *Dhx15* regulates zebrafish definitive hematopoiesis through the unfolded protein response pathway. *Cancer Sci*. 2021;112:3884-3894. <https://doi.org/10.1111/cas.15002>